Low-Temperature Growth of ZnO Nanowire Arrays on p-Silicon (111) for Visible-Light-Emitting Diode Fabrication

ARTICLE *in* THE JOURNAL OF PHYSICAL CHEMISTRY C · AUGUST 2010

Impact Factor: 4.77 · DOI: 10.1021/jp104684m

3 AUTHORS:

Lupan Oleg
University of Central Florida
136 PUBLICATIONS **3,547** CITATIONS
SEE PROFILE

Thierry Pauporté
Chimie ParisTech
163 PUBLICATIONS **4,706** CITATIONS
SEE PROFILE

Bruno Viana
École nationale supérieure de chimie de P…
386 PUBLICATIONS **5,532** CITATIONS
SEE PROFILE

Low-Temperature Growth of ZnO Nanowire Arrays on p-Silicon (111) for Visible-Light-Emitting Diode Fabrication

O. Lupan,[†,§] T. Pauporté,*[,†] and B. Viana[‡]

Laboratoire d'Electrochimie, Chimie des Interfaces et Modélisation pour l'Energie (LECIME), UMR 7575 CNRS, Chimie ParisTech, 11 rue P. et M. Curie, 75231 Paris cedex 05, France, and Laboratoire de Chimie de la Matière Condensée de Paris, UMR 7574-CNRS-ENSCP-UPMC, 11 rue P. et M. Curie, 75005 Paris, France

Received: May 21, 2010; Revised Manuscript Received: July 30, 2010

We report on the successful growth of homogeneous and well-covering ZnO nanowire arrays at a low temperature (90 °C) directly on a p-type Si(111) wafer by an electrochemical method. The wires were self-standing and vertically oriented. Room-temperature micro-Raman and photoluminescence emission analyses showed the high global structural and optical quality of the material with a low density of deep defects. The ZnO nanowires of the heterostructure were contacted with a transparent ITO electrode, and a light-emitting diode was fabricated. The device current−voltage curve had a rectification magnitude of about 20 at 2.5 V. The threshold forward voltage was low at 1.4 V. The device emitted a broad visible band centered at 590 nm at room temperature under forward bias. According to the energy band diagram of the junction, the emission has been assigned possibly to Si hole injection to near-interfacial ZnO deep levels, followed by the radiative recombination with electrons of the ZnO conduction band.

1. Introduction

Zinc oxide is a n-type semiconductor with a large band gap of 3.37 eV, a large exciton binding energy of 60 meV, and a wurtzite hexagonal crystallographic structure. ZnO can be grown as individual or arrays of one-dimensional nanostructures that exhibit superior and additional properties compared with bulk and thin films due to a large surface-to-volume ratio, an inherent anisotropy, and quantum confinement of charge carriers.[1−3] These nanostructures have attracted much attention owing to their potentiality for many applications, such as solar cells,[3−5] superhydrophilic−superhydrophobic surfaces,[6,7] nanosensors,[8] field-emission[9] and electroluminescent devices,[10,11] and nano-lasers.[12]

The use of nanowire (NW) arrays as emitting layers in light-emitting diodes has been shown to be of special interest compared to thin-film-based devices.[11,13] A marked performance improvement is expected from the nanostructure because the nanowires can act as direct waveguides and favor light extraction without the use of lens and reflectors. Moreover, the use of nanowires avoids the presence of grain boundaries, and then the emission efficiency can be boosted by the absence of nonradiative recombinations at the joint defects. The fabrication of NW LEDs based on ZnO p−n homojunctions is very difficult to achieve due to self-compensation by native donor defects. The synthesis of stable, well-conducting, and reproducible p-ZnO still requires a lot of research. However, interesting alternatives are heterostructures in which ZnO nanowires are the n-type emitter contacted to another semiconductor with a different band gap as the p-type material.[11,13−21] Following this scheme, the growth of ZnO nanostructured layers on a p-Si wafer is especially attractive for the well-known advantages of this single-crystalline substrate and its potential applications in Si-based optoelectronic integrated circuits (OEICs).[14−24]

We report on the use for the first time of electrodeposition (ECD) for ZnO NWs/p-Si heterojunction fabrication. ECD has been chosen as a low-temperature growth method of ZnO nanowires that can be implemented for large-scale production.[25] The technique is of utmost interest for the fabrication of optoelectronic devices notably because the grow process involves the exchange of electrons from the substrate and this insures a very good electrical contact between the ZnO nanowires and the substrate (here, the p-type Si). The growth of homogeneous n-ZnO NW arrays has been achieved directly on p-Si(111). By developing a procedure to impede the oxidation of the silicon wafer substrate after the etching steps, we have successfully grown dense arrays of ZnO nanowires of high structural quality characterized by a strong photoluminescence in the UV due to exciton recombination and a very weak emission in the visible wavelength region due to intrinsic deep structural defects. The prepared heterojunctions were integrated in an LED heterostructure. The p−n diodes had a typical rectifying behavior, and visible electroemission could be observed at room temperature under forward bias polarization.

2. Experimental Section

The ZnO NW arrays were grown on highly boron-doped p-type Si(111) substrates with an electrical resistivity of 0.03 Ω·cm (purchased from ACM, Applications Couches Minces, France). The silicon substrates were platelets cut from a 300 μm thick Si wafer with an initial diameter of 3 in. Before electrodeposition, the Si substrates were sequentially cleaned by using three steps: first, a solvent cleaning was done in a warm acetone bath (50−53 °C) for 10 min and in methanol at room temperature, then Si was treated by the RCA-1 cleaning procedure,[26] and, finally, it was dipped in HF (2%) during 120 s just before starting the growth. The Si substrate was mounted

* To whom correspondence should be addressed. Tel: (33)1 55 42 63 83. Fax: (33)1 44 27 67 50. E-mail: thierry-pauporte@chimie-paristech.fr.
† UMR 7575 CNRS.
‡ UMR 7574-CNRS-ENSCP-UPMC.
§ On leave from Department of Microelectronics and Semiconductor Devices, Technical University of Moldova, 168 Stefan cel Mare Blvd., Chisinau, MD-2004, Republic of Moldova.

10.1021/jp104684m
Published on Web 08/16/2010

in a static working electrode (WE) contacted to a copper tape support with In−Ga eutectic. The WE was fixed, and the deposition solution was stirred at a constant speed of 300 rpm with a magnetic barrel. The reference electrode (RE) was a saturated calomel electrode (SCE) with a potential at +0.25 V versus NHE (normal hydrogen electrode). Many different growth potentials were tested. The best results in terms of homogeneity and quality of the layer are presented here, that is, for −1.05 V versus SCE. The deposition bath was a mixture of 0.1 M KCl and 0.2 mM $ZnCl_2$ saturated with molecular oxygen, and the growth temperature was 90 °C.[27] The growing process was stopped after 100 min, corresponding to a total electrical charge exchanged of 6.4 $C \cdot cm^{-2}$.

The samples were observed with a high-resolution Ultra 55 Zeiss FEG scanning electron microscope at an acceleration voltage of 10 kV. X-ray diffraction (XRD) patterns were recorded with a Siemens D5000 apparatus operated at 40 kV and 45 mA using the Cu Kα radiation with $\lambda = 1.5406$ Å and a rotating sample holder. The micro-Raman spectra of the ZnO NW arrays were measured using a Horiba Jobin-Yvon LabRam IR system in a backscattering configuration. The 632.8 nm line of a He−Ne laser was used for off-resonance excitation with less than 4 mW of power at the sample. The sample photoluminescence was measured at room temperature with an excitation source at 266 nm provided by a YAG:Nd quadrupled frequency laser source. Prior to device fabrication, the heterojunction was annealed for 1 h at 200 °C in air. The device assembly was maintained by a bulldog clip and polarized with a Keitley 2400 sourcemeter. Its electroluminescence (EL) was collected by an optical fiber connected to a CCD Roper Scientific detector (cooled Pixis 100 camera) coupled with a SpectraPro 2150i monochromator. The monochromator focal lens was 150 mm; a grating of 300 gr/mm blazed at 500 nm was used in order to record the emission of the ZnO in the whole near-UV−visible range.

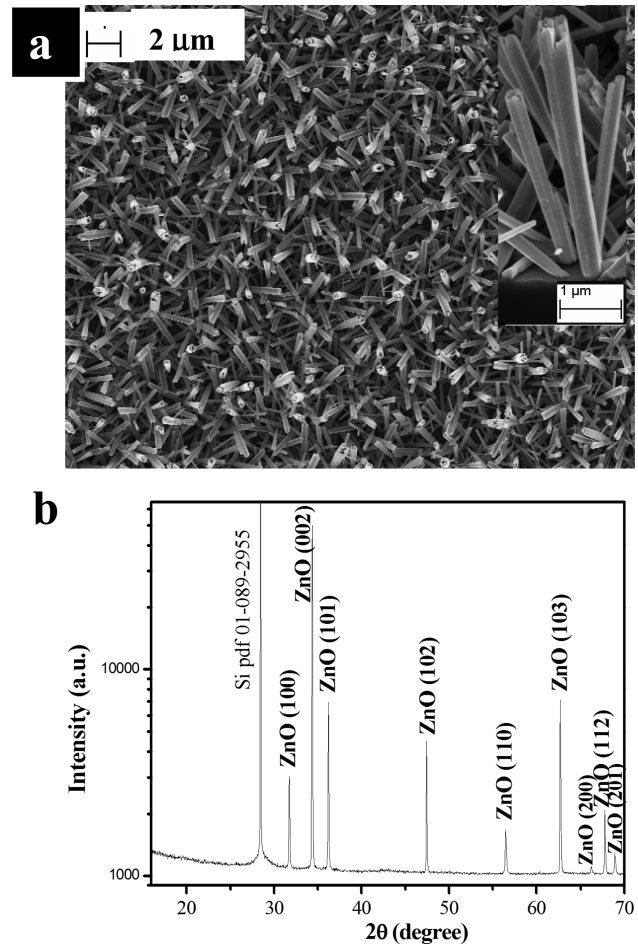

Figure 1. (a) FESEM top view of the ZnO NW array electrodeposited on p-Si(111) (inset: side zoom view). (b) XRD pattern of an as-grown sample.

3. Results and Discussion

The ZnO NW layers were deposited cathodically at a low temperature (90 °C) in the absence of either a seed-layer or a catalyst. The electrochemical reaction occurring on the p-Si(111) electrode was the electroreduction of molecular oxygen dissolved in the bath, which produced hydroxyl ions and generated the ZnO wires by chemical reaction with dissolved Zn(II) ions.[27,28] Molecular oxygen was chosen as the dissolved precursor because it produces only hydroxide ions by reduction and no byproduct that may progressively pollute the deposition bath. Because of oxygen bubbling, the deposition bath had oxidizing properties.[29] To avoid, or at least to limit, the formation of a thin amorphous silica layer at the electrode surface, immediately after the final etching, the working electrode was connected to an auxiliary platinum electrode that was prepolarized at the deposition negative potential of −1.05 V/SCE. The working electrode was then rapidly placed in the cell and then the auxiliary electrode removed. High-resolution SEM views of the ZnO deposited layer are presented in Figure 1a. The substrate was homogeneously well-covered by an array of self-standing ZnO wires with the tendency to grow normal to the surface. Their diameter ranged between 100 and 200 nm, and their mean length was 2.8 μm. The wire density was 12−14 $NW \cdot \mu m^{-2}$. The side view in Figure 1a illustrates that the ZnO nanowires were directly attached to the p-Si(111) substrate. The general aspect of the deposit was unchanged after an annealing treatment at 200 °C during 1 h in air. The crystallographic structure and orientation of ZnO wires on Si substrates were studied by XRD. The pattern in Figure 1b is indexed with the various diffraction peaks of the wurtzite phase of ZnO. The ZnO(002) is the most intense, and the comparison of the pattern with a ZnO powder standard (JCPDS 036-1451 card) shows a preferential orientation with the *c* axis perpendicular with the substrate, in good agreement with the verticality of the *c*-axis-elongated nanowires on SEM views. The fwhm (002) for the as-grown sample was 0.09°. Annealing the sample improved the crystalline quality of the wires because the XRD peak intensities increased by 15% and the fwhm was reduced to 0.08°. The lattice parameter *d* (002) of ECD ZnO was 2.609 and 2.603 Å before and after annealing at 200 °C, respectively. The latter value is comparable to the 2.602 Å reported in the unstressed ZnO bulk.[1] The lattice parameters *c* and *a* were obtained for the as-grown sample using standard relations:[30] $c = 5.22 \pm 0.01$ Å and $a = 3.247 \pm 0.005$ Å. The measured value of the *c*/*a* ratio for each sample was 1.607, in agreement with value for bulk ZnO at 1.602.[1]

Micro-Raman scattering was used to study the phase and the quality of the ZnO NWs.[31] Figure 2a shows Raman spectra measured at room temperature in a backscattering geometry for an as-grown and an annealed sample. From both as-grown and air-annealed NW arrays, if we except the Si substrate emission peaks, all the observed three peaks are related to the ZnO wurtzite phase: the characteristic and strong E_2 (high) and E_2 (low) modes at 438 and 100 cm^{-1}, in addition to a second-order $2E_2$ mode at 333 cm^{-1}. The higher intensity of the E_2 mode peaks in the annealed sample indicates that the crystalline quality of ZnO was improved by the treatment. The quality and

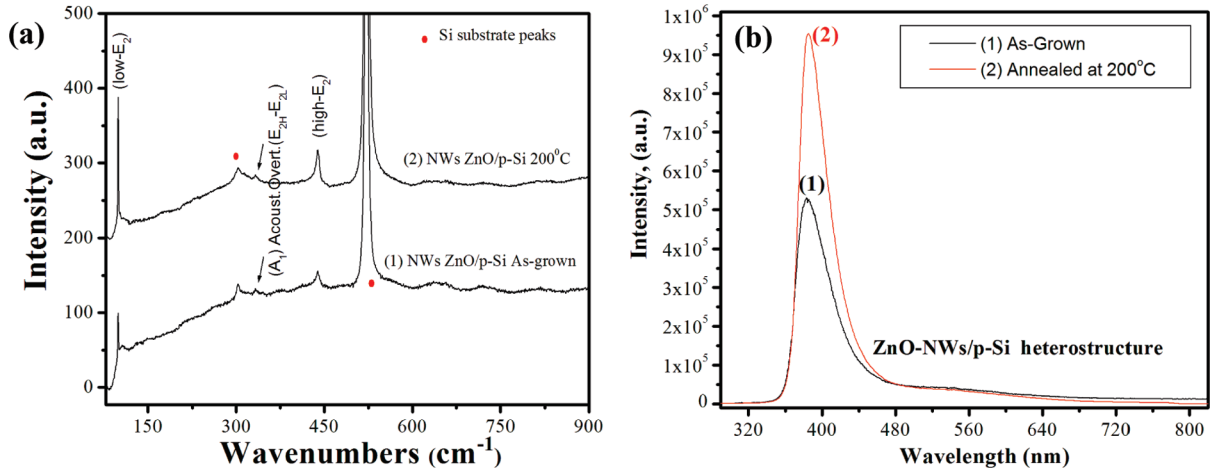

Figure 2. (a) Micro-Raman spectra from as-grown ZnO NW arrays on p-Si(111) (1) and from the same sample after annealing for 1 h at 200 °C in air (2). (b) PL spectrum of an as-prepared sample (curve 1) and of a sample annealed at 200 °C for 1 h in air (curve 2). All spectra were measured at $T = 300$ K.

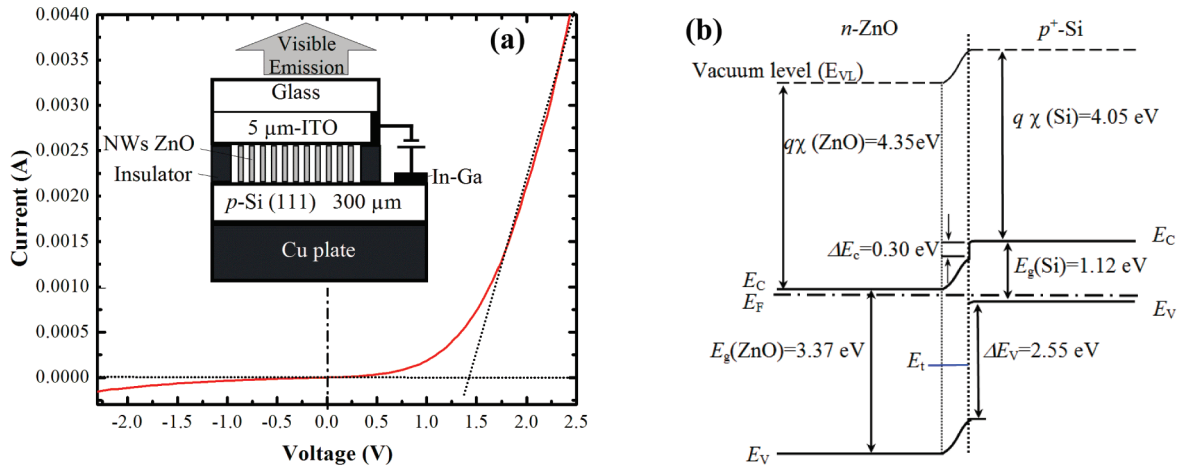

Figure 3. (a) Room-temperature $I-V$ curve of the ZnO/p-Si heterojunction. The inset shows the device structure. (b) The energy band diagram of the heterojunction under thermal equilibrium.

emission properties of the deposited material were also investigated by room-temperature photoluminescence (PL) measurements. The PL spectrum of the as-grown ZnO nanowires in Figure 2b, curve 1, exhibits a strong near band edge UV-PL emission and a weak emission centered at 520 nm due to deep defects classically described as oxygen vacancies at this wavelength.[2,28,32] The UV emission is broad and has a maximum at 384 nm at room temperature. According to previous studies, the UV emission can be assigned to free exciton (FX) and to longitudinal optical replicas of the free excitions (FX-LO), which give rise to an emission tail at high wavelengths.[28,33−35] The intensity ratio I_{UV}/I_{Vis} of the UV and visible emissions is a measure of the quality of the prepared ZnO in terms of native defect concentration.[28,32] The ratio for the as-grown material was rather high at 13, demonstrating the very good quality of the initial material. After annealing (Figure 2b, curve 2), the intensity of the near band-gap luminescence markedly increased by 1.8 and the UV emission was narrowed possibly due to a decrease in the charge carrier concentration. The visible part remained unchanged, and the intensity ratio between the UV and visible emissions was increased up to 24. The thermally treated layer was of high structural quality with a low intrinsic defect concentration.

The annealed ZnO NWs/p-Si heterostructures were used to fabricate a light emitting diode structure, as illustrated in the schematic of Figure 3a. The top of the ZnO wires was contacted with an ITO layer deposited on a transparent glass sheet. The ohmicity of the ITO contact with ZnO has been described in the literature[36] and checked here. The top TCO (transparent conducting oxide) plate and the uncovered Si wafer were spaced by a thin polymer elastic polymer insulator (Surlyn) to avoid the direct contact between the two layers and breakdown of NWs. The Si layer was contacted with In−Ga eutectic. The current−voltage ($I-V$) characteristic in Figure 3a illustrates the rectifying behavior of the prepared device. The current increased rapidly under forward bias and was blocked under reverse bias. The rectification magnitude was about 20 at 2.5 V. The forward threshold voltage of our diode structure, defined by extrapolating the linear fit of the high current regime at $I = 0$, was about 1.4 V. The rectifying behavior is predicted from the theoretical energy band diagram of the n-ZnO/p-Si heterojunction under thermal equilibrium. In Figure 3b, the diagram has been drawn by using data extracted from the literature,[37] and we suppose that ZnO is directly in contact with Si, without any interfacial layer. The heterojunction exhibits a type II band alignment determined by the Anderson's model.[38] In the diagram, the valence band offset is 2.55 eV and that of the conduction band is 0.3 eV.[37] Because of the large difference in ΔE_V and ΔE_C, the energetic barrier for electrons is much lower than that for holes.

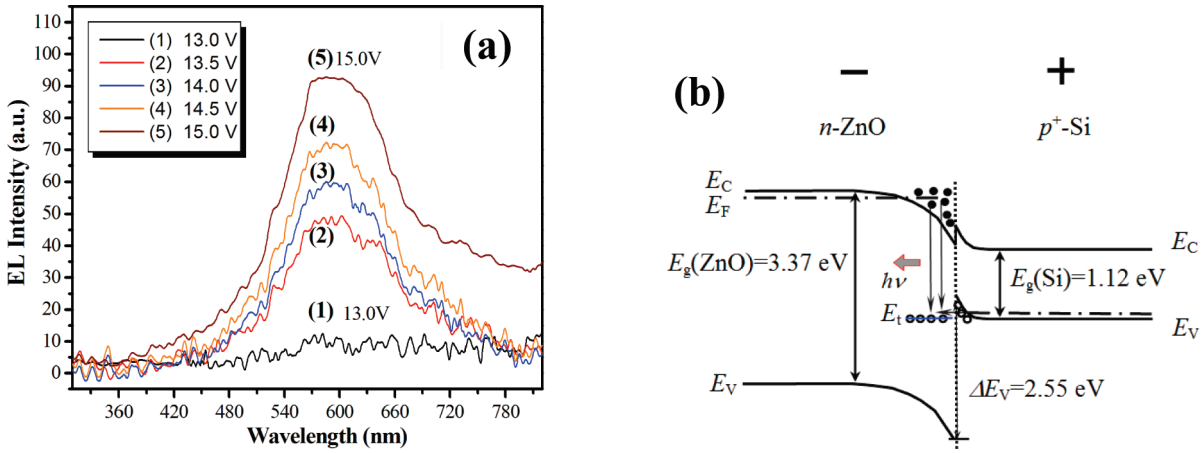

Figure 4. (a) RT-EL spectra of the n-ZnO NW/p-Si heterojunction structure at various forward bias voltages. (b) The energy band diagram of the heterojunction under forward bias polarization and visible emission mechanism.

The room-temperature electroluminescence (EL) emission of the LED structure was studied over a large applied voltage range. No electroluminescence was detected under reverse bias. Above a forward bias of 13 V, the emission was dominated by a visible peak (Figure 4a). The obtained spectra clearly differed from the PL spectra because no near band-edge UV emission arised from ZnO despite the very good quality of the ZnO material. The absence of UV emission can be assigned to the large energetic barrier for hole injection from Si to the valence band of ZnO (Figure 3b). The orange-red emission was centered at about 590 nm (2.1 eV) and rapidly increased with the applied forward voltage (Figure 4a). No straightforward explanation of the emission can be given because the EL spectra clearly differ from the PL ones at room temperature. However, EL is an interfacial process because the emission is generated near the p−n junction, whereas PL probes the bulk wire material. The defects at the origin of the radiative recombinations were not detected by PL because this method probes the bulk and the near surface of the NWs and the contribution of interfacial defects on the PL emission is negligible. Because the Si substrate was of high structural quality and it was carefully etched, we can suppose that defects were introduced in ZnO upon deposition notably due to the lack of crystallographic continuity between Si and ZnO. Despite all the special care attached to the substrate preparation, it is also probable that the Si surface was not kept free of a native thin SiO_x layer before growing ZnO. The presence of a thin silica layer may have disturbed the crystallographic quality of the near-interfacial deposited ZnO. A visible emission involving defects in an amorphous SiO_x interlayer cannot be ruled out, but such a mechanism is not supported by luminescence data on SiO_x from the literature.[39,40] A possible mechanism of recombination involving local deep defect states is illustrated in Figure 4b. Under forward polarization, holes are transferred from the Si valence band (E_v) into ZnO deep states (noted E_t) and then partly recombinate radiatively with the electrons localized in the conduction band (E_c) of ZnO. We can note that a similar defect-related orange-red EL emission was reported in the literature for dense n-ZnO/p-Si heterojunctions prepared by a metal organic chemical vapor deposition technique.[12] However, the exact description of the phenomenon remains difficult due to the localized process of charge recombinations near the interface that generate the light emission by charge injection and recombinations.

4. Conclusion

We have successfully grown dense and well-covering arrays of ZnO nanowires on p-type Si(111) wafers by an electrochemical method. The wires were self-standing, vertically oriented, and directly attached to the Si substrate. The synthesis was performed at a low temperature, and a procedure was developed that allowed the fine control of the initial substrate state and ZnO growth. The deposited material was of high structural quality with a low density of deep defects. After integration in an LED structure, the nanostructured heterojunctions presented a typical rectifying $I-V$ characteristic of p−n junction. A visible electroluminescence centered at 590 nm (2.1 eV) was detected for a forward bias higher than 13 V. The emission has been discussed in the light of literature data, and it has been suggested as possibly due to deep local states localized near the interface in the deposited material. The traps would permit the radiative charge recombination between holes coming from p-Si and electrons from n-ZnO. Our results open up new possibilities to integrate silicon-based optoelectronic devices, such as visible LEDs, with standard Si ultra-large-scale integrated technology.

Acknowledgment. This research was performed with the financial support of the C-nano Ile-de-France program (nanoZnO-LED Project) for funding Dr. O. Lupan's post-doctoral fellowship and a part of this work. P. Aschehoug (LCMCP, ENSCP, Paris) is acknowledged for PL measurements.

References and Notes

(1) Ozgur, U.; Alivov, Y. I.; Liu, C.; Teke, A.; Reshchikov, M. A.; Dogan, S.; Avrutin, V.; Cho, S. J.; Morkoç, H. *J. Appl. Phys.* **2005**, *98*, 041301.

(2) Pauporté, T. Design of Solution-Grown ZnO Nanostructures in Toward Functional Nanomaterials. In *Lecture Notes in Nanoscale Science and Technology*; Wang, Z. M., Ed.; Springer: New York, 2009; Vol. 5, Chapter 2, pp 77−127.

(3) Könenkamp, R.; Word, R. W.; Godinez, M. *Nano Lett.* **2005**, *5*, 2005.

(4) Law, M.; Greene, L. E.; Johnson, J. C.; Saykally, R.; Yang, P. *Nat. Mater.* **2005**, *4*, 455–459.

(5) Lupan, O.; Guérin, V. M.; Tiginyanu, I. M.; Ursaki, V. V.; Chow, L.; Heinrich, H.; Pauporté, T. *J. Photochem. Photobiol., A* **2010**, *211*, 65–73.

(6) Badre, C.; Pauporté, T. *Adv. Mater.* **2009**, *21*, 697–701.

(7) Pauporté, T.; Bataille, G.; Joulaud, L.; Vermersch, J. F. *J. Phys. Chem. C* **2010**, *114*, 194–202.

(8) Wang, X. D.; Summers, C. J.; Wang, Z. L. *Nano Lett.* **2004**, *4*, 423–426.

(9) Tseng, Y. K.; Huang, C. J.; Cheng, H. M.; Lin, I. N.; Liu, K. S.; Chen, I. C. *Adv. Funct. Mater.* **2003**, *13*, 811–814.

(10) Jeong, M. C.; Oh, B. Y.; Ham, M. H.; Myoung, F. *Appl. Phys. Lett.* **2006**, *88*, 202105.

(11) Lupan, O.; Pauporté, T.; Viana, B. *ACS Appl. Mater. Interfaces* **2010**, *2*, 2083–2090.

(12) Huang, M. H.; Mao, S.; Feick, H.; Yan, H.; Wu, Y.; Kind, H.; Weber, E.; Russo, R.; Yang, P. *Science* **2001**, *292*, 1897–1899.

(13) Jeong, M. C.; Oh, B. Y.; Ham, M. H.; Lee, S. W.; Myong, J. M. *Small* **2007**, *3*, 568–572.
(14) Ye, J. D.; Gu, S. L.; Gu, S. M.; Zhu, S. M.; Liu, W.; Zhang, R.; Shi, Y.; Zheng, Y. D. *Appl. Phys. Lett.* **2006**, *88*, 182112.
(15) Sun, H.; Zhang, Q. F.; Wu, J. L. *Nanotechnology* **2006**, *17*, 2271–2274.
(16) Tan, S. T.; Sun, X. W.; Zhao, J. L.; Iwan, S.; Cen, Z. H.; Chen, T. P.; Ye, J. D.; Lo, G. Q.; kwong, D. L.; Teo, K. L. *Appl. Phys. Lett.* **2008**, *93*, 013506.
(17) Hsieh, Y. P.; Chen, H. Y.; Lin, M. Z.; Shiu, S. S.; Hofmann, M.; Chern, M. Y. *Nano Lett.* **2009**, *9*, 1839–1843.
(18) Wang, F. F.; Cao, L.; Liu, R. B.; Pan, A. L.; Zou, B. S. *Chin. Phys.* **2007**, *16*, 1790–1795.
(19) Li, X.; Zhang, B.; Dong, X.; Zhang, Y.; Xia, X.; Zhao, W.; Du, G. *J. Lumin.* **2009**, *129*, 86–89.
(20) Kim, D. C.; Han, W. S.; Cho, H. K.; Kong, B. H.; Kin, H. S. *Appl. Phys. Lett.* **2007**, *91*, 231901.
(21) Klason, P.; Rahman, M. M.; Hu, Q. H.; Nur, O.; Turan, R.; Willander, M. *Microelectron. J.* **2009**, *40*, 706–710.
(22) Rout, C. S.; Rao, C. N. R. *Nanotechnology* **2008**, *19*, 285203.
(23) Zhang, Y. W.; Li, X. M.; Yu, W. D.; Gao, X. D.; Gu, Y. F.; Yang, C.; Zhao, J. L.; Sun, X. W.; Tan, S. T.; Kong, J. F.; Shen, W. Z. *J. Phys. D* **2008**, *41*, 205105.
(24) Sun, M. H.; Zhang, Q. F.; Sun, H.; Zhang, J. Y.; Wu, J. L. *J. Vac. Sci. Technol., B* **2009**, *27*, 618–621.
(25) Rappich, J.; Fahoume, M. *Thin Solid Films* **2005**, *487*, 157–161.
(26) Kern, W. A.; Puotinen, D. A. *RCA Rev.* **1970**, *31*, 187–197.
(27) Goux, A.; Pauporté, T.; Lincot, D. *Electrochim. Acta* **2006**, *51*, 3168–3172.
(28) Pauporté, T.; Jouanno, E.; Pellé, F.; Viana, B.; Aschehoung, P. *J. Phys. Chem. C* **2009**, *113*, 10422–10431.
(29) Konenkamp, R.; Word, R. C.; Dosmailov, M. *J. Appl. Phys.* **2007**, *102*, 056103.
(30) Lupan, O.; Pauporté, T.; Chow, L.; Viana, B.; Pellé, F.; Roldan Cuenya, B.; Ono, L. K.; Heinrich, H. *Appl. Surf. Sci.* **2010**, *256*, 1895–1907.
(31) Chow, L.; Lupan, O.; Heinrich, H.; Chai, G. *Appl. Phys. Lett.* **2009**, *94*, 163105.
(32) Chen, Y.; Bagnall, D. M.; Koh, H.-j.; Park, K.-t.; Hiraga, K.; Zhu, Z.; Yao, T. *J. Appl. Phys.* **1998**, *84*, 3912–3918.
(33) Meyer, B. K.; Alves, H.; Hofmann, D. M.; Kriegseis, W.; Forster, D.; Bertram, F.; Christen, J.; Hoffmann, A.; Strassburg, M.; Dworzak, M.; Haboeck, U.; Rodina, A. V. *Phys. Status Solidi B* **2004**, *241*, 231–260.
(34) Loewenstein, T.; Sann, J.; Neumann, C.; Meyer, B. K.; Schlettwein, D. *Phys. Status Solidi A* **2008**, *205*, 2382–2387.
(35) Cui, J. B. *J. Phys. Chem. C* **2008**, *112*, 10385–10388.
(36) Chen, C. H.; Chang, S. J.; Chang, S. P.; Li, M. J.; Chen, I. C.; Hsueh, T. J.; Hsu, C. L. *Appl. Phys. Lett.* **2009**, *95*, 223101.
(37) Chen, P.; Ma, X.; Yang, D. *J. Appl. Phys.* **2007**, *101*, 053103.
(38) Jeong, I. S.; Kim, J. H.; Im, S. *Appl. Phys. Lett.* **2003**, *83*, 2946–2948.
(39) Skuja, L. *J. Non-Cryst. Solids* **1994**, *179*, 51–69.
(40) Tohmon, R.; Shimogaichi, Y.; Mizuno, H.; Ohki, Y.; Nagasawa, K.; Hama, Y. *Phys. Rev. Lett.* **1989**, *62*, 1388–1391.

JP104684M